

Electronic Properties of Ru/Pt(111) Alloy Surface: A Theoretical Study of H₂O Adsorption

Dae-Bok Kang* and Choon-Kee Lee

Department of Chemistry, Kyungshung University, Pusan 608-736, Korea

Received August 30, 1999

The electronic and chemical properties of the surface Pt and Ru atoms in the Pt-Ru alloy have been investigated by means of extended Hückel calculations. An electron transfer occurs from Ru to Pt, resulting in an increased electron density on the surface Pt atoms. The transfer is found to be larger toward Pt atoms out of contact with Ru. The calculated electronic perturbation of the water molecule is similar when it is adsorbed either on the Pt site or on the Ru site in the alloy. However, the water adsorption strength is much smaller in the former case, since the lone-pair donations are reduced relative to the latter case. This is essentially due to a larger closed-shell repulsive interaction between $1b_2$ (H₂O) and d_{yz} (Pt).

Introduction

It is well known that bimetallic systems show their improved catalytic properties relative to the pure metals. Numerous experimental studies have indicated that alloying two metals modifies their electronic and chemical properties.¹⁻¹² It is of interest to study the changes that occur in the electronic properties of the transition metals when they are alloyed with another metal. We chose the Ru/Pt(111) alloy system in this work. The H₂O molecule was chosen for studying the chemisorptive properties. This system is an excellent example by which to address the problem of the electronic effects in transition metal alloys and of their influence on adsorption properties. A recent molecular orbital study showed that H₂O is strongly attracted to substitutional Ru in Pt surfaces and dissociates with a low barrier compared to when it is on Pt.¹³

In the present paper we examine the electronic properties of the Pt-Ru alloy surface by means of extended Hückel calculations in order to explain its behavior toward water adsorption and catalytic reactions. Our focus is on understanding how different are the chemisorptive properties of the surface Pt and Ru atoms in the Pt-Ru alloy, and on comparing them with those of the Pt atoms in the pure Pt(111) surface.

Theoretical Model

Our calculations are based on the extended Hückel (EH) theory. Two kinds of method were used. One is molecular and the other is of the periodic type. The former allows one to obtain the electron transfers between the molecular orbitals of the adsorbate and the surface. The latter allows the study of the adsorption of small molecules such as CO and H₂O on transition metal surfaces. For larger molecules this method is less convenient since large surface unit cells must be chosen in order to avoid interactions between the adsorbates. With this method, most of interpretations can be done in terms of density of states (DOS) and crystal orbital overlap population (COOP) curves.

All atomic parameters used in our calculations are listed in Table 1. No experimental data exist for the alloy system studied here. Consequently, we have taken the standard values of the exponents from the literature.¹⁴ The H_{ii} values which represent the energy of the atomic orbitals are those found in ref. 13 where the parameters were adjusted from the standard values¹⁵ so as to reduce orbital polarizations (charge transfers) for diatomic fragments.

For the periodic band calculations a two-layer slab was used. The unit cell contains four metal atoms per layer and one adsorbate molecule (see Figure 1b). This model forms a $p(2 \times 2)$ H₂O substructure in a coverage of 1/4 where the interactions between the adsorbates are reduced. For the cluster molecular orbital (MO) calculations the pure Pt(111) surface is modeled by a cluster of 18 atoms arranged in two layers (Figure 1a). For the Pt-Ru alloy, as shown in Figure 1a, a Ru atom is placed substitutionally in the surface plane leading to the RuPt₁₇ cluster. The metal-metal distance has been kept at 2.77 Å as in pure Pt. We use a fixed water geometry: O-H bond distance = 0.96 Å and H-O-H bond angle = 104.5°. It is assumed that the oxygen from H₂O is adsorbed on the top of a surface atom and its molecular plane is perpendicular to the surface. Tilting of the molecular plane toward the surface induces only a little change of binding energy as the oxygen atom is anchored at the same posi-

Table 1. Parameters used for the calculations

Atom	Orbital	H_{ii}^a (eV)	ζ_1^b	ζ_2^b	C_1^c	C_2^c
Ru	5s	-9.37	2.08			
	5p	-6.11	2.04			
	4d	-10.5	5.38	2.30	0.5340	0.6365
Pt	6s	-10.5	2.554			
	6p	-6.46	2.554			
	5d	-11.1	6.013	2.696	0.6334	0.5513
O	2s	-26.98	2.275			
	2p	-12.12	2.275			
H	1s	-12.1	1.3			

^aDiagonal Hamiltonian matrix elements. ^bSlater exponents. ^cCoefficients in double ζ expansion.

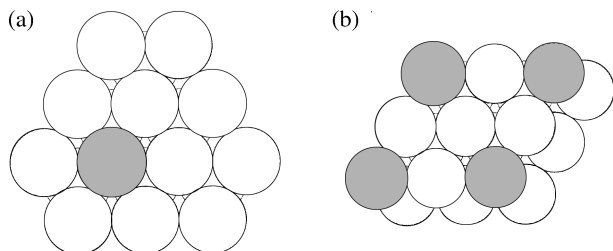


Figure 1. Two-layer cluster (a) and slab (b) models of the Pt-Ru alloy used for the calculations. The dark circles indicate the substitutional Ru atoms in the Pt(111) surface.

tion as in the upright configuration.

Electronic Properties of Pure Pt and Pt-Ru Alloy Surfaces

We have performed the periodic slab calculations by considering the (111) surface of the Pt-Ru alloy as being ordered face-centered cubic (fcc). The surface structure of the alloy is not known, so we have assumed the segregation of Pt at the surface which only contains Pt atoms. The top layer has the Pt₃Ru composition with a $p(2 \times 2)$ ordered Ru lattice in the (111) Pt plane, whereas the second one has pure Pt atoms (see Figure 1b).

For the alloy surface, the Fermi level (E_F) shifts toward higher energy by 0.1 eV compared with the pure Pt. There is an electron transfer from the less electronegative metal Ru to the Pt atoms. The Pt atoms out of contact with a Ru atom gain more electrons than the others (0.42 vs. -0.03 e^- /atom). This will be explained below in more detail. The transfer may be somewhat excessive. This trend is inherent to the EH method. Hence this method is well suited for the understanding of the chemical interactions on large systems and for the qualitative comparison of the molecular binding at different adsorption sites to be studied in the following section.

If one analyzes the electronic structures of the metal d orbitals given in Figure 2, one notices how they change after alloying. The shape of the DOS projected on Pt d orbitals does not change much when Pt is alloyed with Ru. However, the Fermi level is shifted up in the alloy; the main d part of Pt becoming more distant from the Fermi level. The peak which lies on the top of the d band exhibits a large contribution of the Ru d orbitals (Figure 2b). At the very bottoms of the valence bands, the valence s atomic contributions are large.

The d-d interactions are more attractive in the alloy than in pure Pt. This is illustrated by the COOP curves of Figure 3 which show the overlap population (0.55) between a Ru atom and the nearest-neighbor Pt atom in the alloy (Figure 3b) and the overlap population (0.49) between the nearest-neighbor metal atoms in the pure Pt (Figure 3a). In the latter figure part of the antibonding interactions is occupied with electrons almost to the top of the d band. In the former, owing to the influence of Ru, a substantial part of the antibonding peaks is pushed above the Fermi level and the resulting interaction is more attractive.

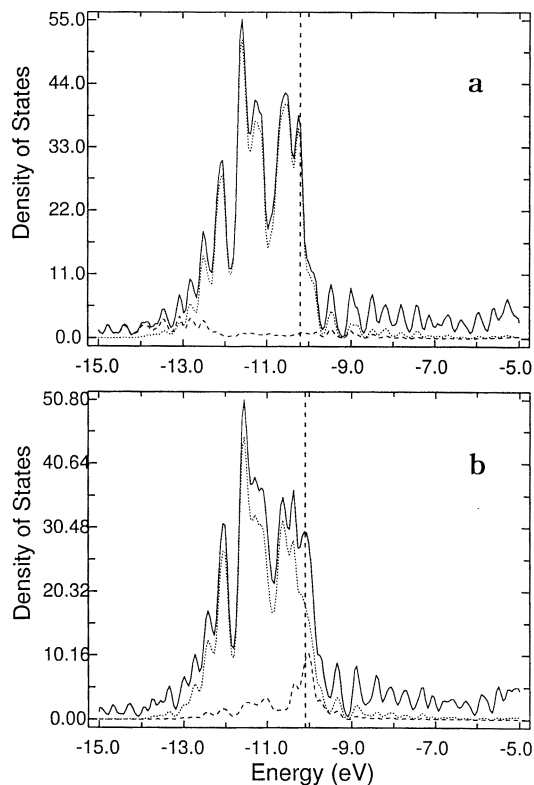


Figure 2. DOS projected on the Pt d (dotted line) and s (dashed line) orbitals in pure Pt (a) and DOS projected on the Pt d (dotted line) and the Ru d (dashed line) orbitals in the alloy (b). The solid line represents the total DOS. The dashed vertical line refers to the Fermi level.

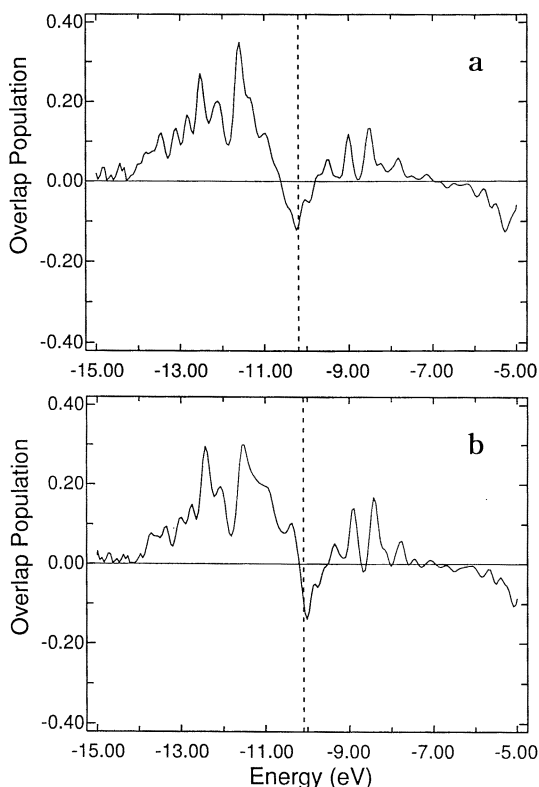


Figure 3. COOP of the Pt-Pt bond in pure Pt (a) and COOP of the Ru-Pt bond in the alloy (b). The dashed vertical line refers to the Fermi level.

This is also reflected in the DOS projected on d orbitals as depicted in Figure 2b. The top of the Pt d band interacts with Ru d which is higher in energy and is pushed below the Fermi level. The fact that part of the d band goes above the Fermi level by interaction with the Ru d orbitals and loses its electrons is compensated by the up-shift of this level and hence the d orbital population of the Pt atoms in contact with Ru does not change much as described above. The Pt orbitals that have the strongest interaction with Ru have the smallest change in their electronic occupation, while those that have little interaction with Ru are more populated by the up-shift of the Fermi level and the electrons lost by Ru. Therefore, the DOS deformation and Fermi level shift caused by alloying are responsible for more electron gain for the Pt atoms not in contact with a Ru atom. This means that the electron transfer from more electropositive Ru atom does not take place only toward its nearest neighbors, but mainly toward the farther Pt atoms. Since the DOS curves of the pure metal orbitals are considerably changed in the alloy, one can understand that alloying Pt with Ru will modify the adsorption properties significantly. This point will be discussed in the next section.

H₂O Adsorption

The structure and reactions of water adsorbed on platinum surfaces are extensively documented experimentally.¹⁶⁻²⁰ Quantum chemical calculations favor the on-top adsorption site compared to the bridge and threefold sites for an H₂O molecule on Pt(111).²¹ The Pt-O bond distance has been found as 1.79 Å for the on-top site. For the adsorption on the Ru site in the Pt alloy, the Ru-O length has been taken at 1.68 Å following ref. 13. These bond lengths are used in our calculations. Since our purpose is to compare H₂O adsorption on the Pt and Ru sites in the Pt-Ru alloy with that on pure Pt, we have considered only the on-top adsorption site. The results are given in Table 2.

The calculated adsorption energies reveal a large difference between the Ru and the Pt sites on the alloy surface

Table 2. Bonding characteristics for H₂O adsorption on Pt(111) and Pt-Ru alloy clusters as modeled in Figure 1^a

	Pt(111)	Pt in alloy	Ru in alloy
Binding energy ^b (eV)	1.78 (1.32)	1.57 (1.16)	2.70 (2.16)
H ₂ O charge	0.73	0.65	0.83
Overlap population			
O-H (0.64) ^c	(0.64)	(0.64)	(0.64)
metal-O	0.59 (0.52)	0.56 (0.51)	0.71 (0.69)
Electron transfer			
loss of 2a ₁	0.07	0.07	0.09
loss of 1b ₁	0.01	0.01	0.06
loss of 3a ₁	0.45	0.45	0.39
loss of 1b ₂	0.22	0.14	0.32

^aIn parentheses are given the results obtained with the periodic band calculations. ^bTaken as the difference: E (adsorbate) + E (substrate) - E (adsorbate/substrate) in eV. A positive value implies a stabilization. ^cValue in free H₂O.

(2.70 and 1.57 eV for Ru and Pt sites in the alloy, respectively, and 1.78 eV for the pure Pt surface), indicative of a markedly stronger H₂O adsorption on the Ru site in the alloy. In order to explain this difference, we have chosen to focus on the interpretations based on the interactions between the molecular orbitals. The bonding between metal atoms in a surface and water molecules is predominantly achieved by H₂O lone-pair donation. The lone-pair bonding to the surface involving overlap with occupied and empty surface orbitals is illustrated schematically in Figure 4. In the case of lone-pair overlap with occupied surface orbitals, the bonding stabilization represented by the downward pointing arrow is reduced by the destabilizing energy required to promote some electrons to the Fermi level via the antibonding counterpart orbitals. In the case of overlap with an empty surface orbital there is no promotion of electrons due to the antibonding counterpart orbitals to the Fermi level and therefore no destabilizing deduction from the bonding stabilization energy. The greater stabilization that occurs for the bonding orbitals when the donor and surface orbitals become closer in energy is explained by a perturbation theory approach.

These two types of interaction just described will occur for each surface band orbital with a non-zero overlap integral with the lone-pair orbitals of H₂O at the adsorption site. The d band, almost filled for pure Pt, interacts both with the lone-pair orbitals 3a₁ and 1b₂ of H₂O. These interactions are depicted in Figure 5. By these interactions, part of the d band is pushed above the Fermi level and loses electrons, which

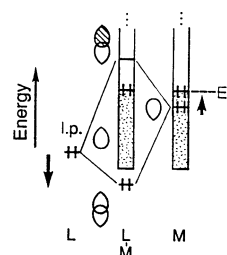


Figure 4. Schematic illustration showing the stabilization of a ligand (L) lone-pair orbital by a metal (M) surface orbital. Note the destabilizing component indicated by the heavy upward pointing arrow. If the metal surface orbital is empty, there will be no destabilizing deduction from the bonding stabilization energy.

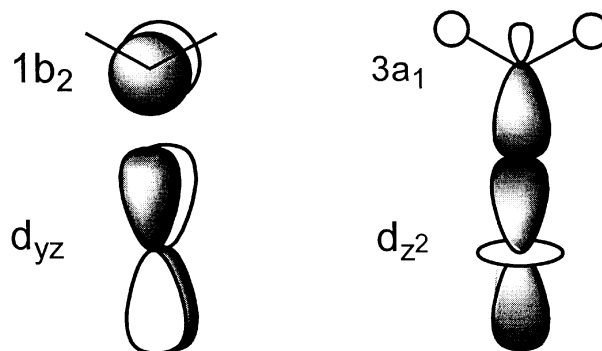


Figure 5. Orbital interactions between H₂O and a surface metal atom in the on-top site.

results in bonding. In the alloy, the Fermi level is higher in energy and the Pt d band is farther from E_F (see Figure 2b); hence a smaller part of this band is pushed above the Fermi level for the adsorption on Pt, which results in weaker bonding. On the contrary, the lone-pair donation interactions with the Ru d band that is located at and near the Fermi level push most part of the d band above the Fermi level, and the antibonding counterparts become empty. This result leads to a considerably high O-Ru bond strength. The larger the part of the d band pushed above E_F , the more stabilizing the water-surface interaction.

Let us now interpret these interactions by the DOS projected on d_{z^2} and d_{yz} metal orbitals appropriated for an interaction with the lone-pair orbitals of H_2O . For energetic

position and symmetry reasons, only the $3a_1-d_{z^2}$ and $1b_2-d_{yz}$ interactions will be considered in this qualitative study of chemisorption. The water $1b_1$ orbital interacts only very little with the d_{xz} orbital because of their poor energy match, and the empty OH σ^* orbitals are too high-lying in energy to interact with the metal d band.

The DOS curves of the two interactions considered are shown in Figures 6-8. The comparison of Figure 7b with Figure 8b shows that the d_{yz} antibonding state is pushed above E_F in the case of the Ru site, whereas it goes just below E_F in the case of the Pt site in the alloy. The d_{z^2} antibonding states are pushed above E_F in all cases. At the same time, the H_2O $1b_2$ and $3a_1$ lone-pair orbitals also show a larger contribution over E_F for the Ru site than for the Pt site

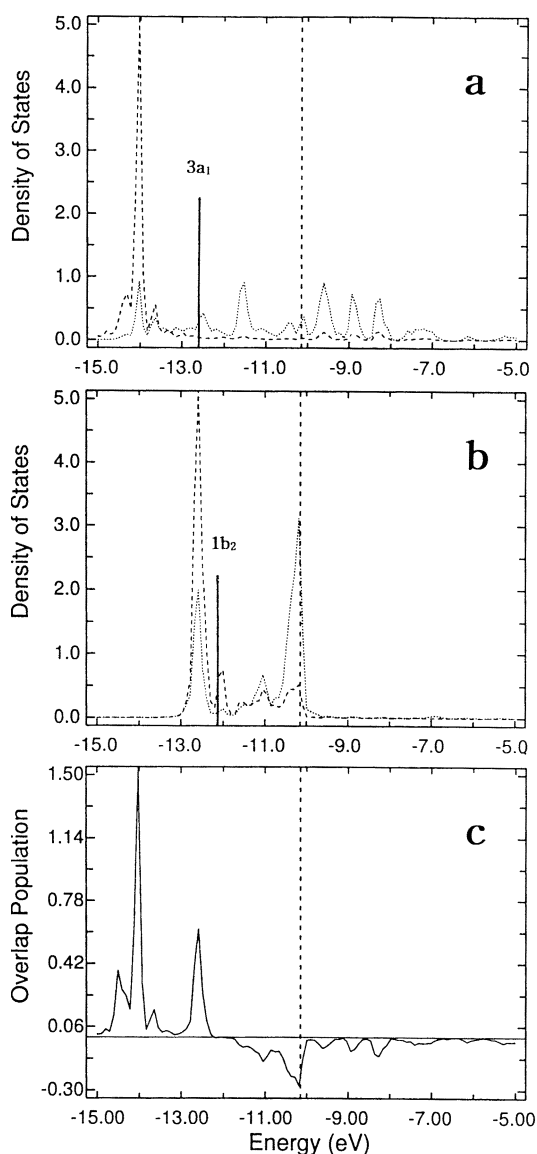


Figure 6. H_2O adsorption on Pt(111): DOS projected on the d_{z^2} (a) and d_{yz} (b) (dotted line) of a Pt atom of the adsorption site and on the $p_z(O)$ (a) and $p_y(O)$ (b) (dashed line) of H_2O , and COOP of the Pt-O bond (c). The vertical bars display the position of $3a_1$ and $1b_2$ orbitals in free H_2O . The dashed vertical line refers to the Fermi level.

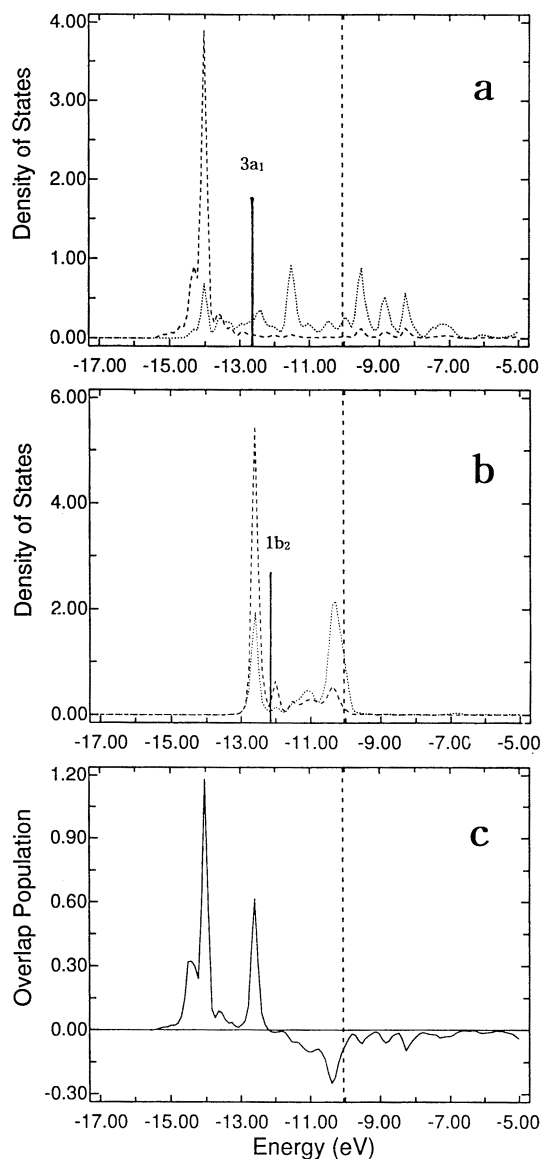


Figure 7. H_2O adsorption on Pt in the alloy: DOS projected on the d_{z^2} (a) and d_{yz} (b) (dotted line) of a Pt atom of the adsorption site and on the $p_z(O)$ (a) and $p_y(O)$ (b) (dashed line) of H_2O , and COOP of the Pt-O bond (c). The vertical bars display the position of $3a_1$ and $1b_2$ orbitals in free H_2O . The dashed vertical line refers to the Fermi level.

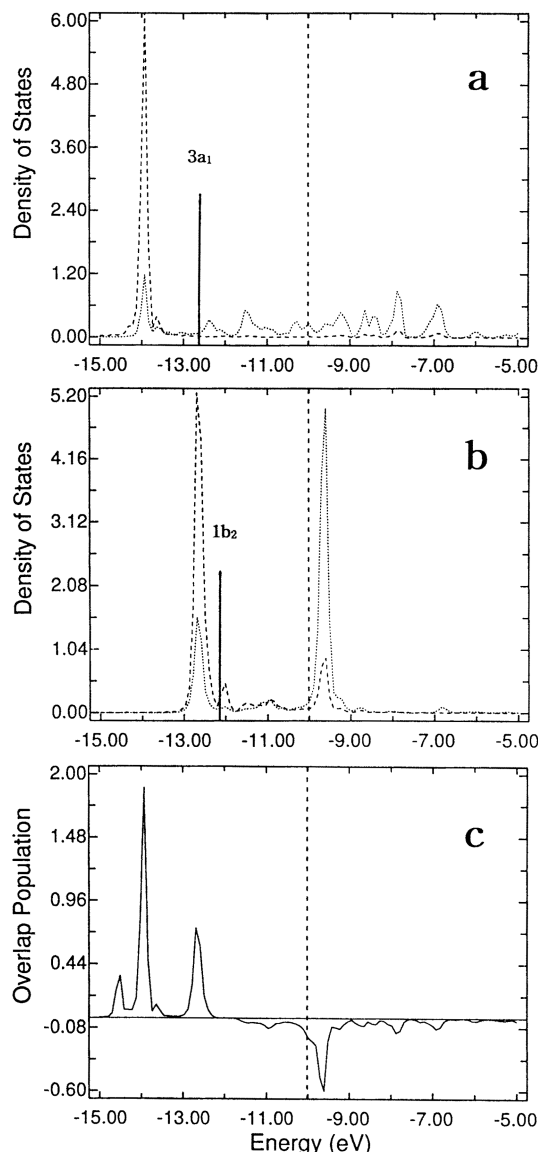


Figure 8. H₂O adsorption on Ru in the alloy: DOS projected on the d_{z^2} (a) and d_{yz} (b) (dotted line) of a Ru atom of the adsorption site and on the p_z (O) (a) and p_y (O) (b) (dashed line) of H₂O, and COOP of the Ru-O bond (c). The vertical bars display the position of $3a_1$ and $1b_2$ orbitals in free H₂O. The dashed vertical line refers to the Fermi level.

in the alloy and hence lose more electrons in the case of the Ru site (0.71 vs. 0.59 e^- in Table 2). Moreover, the overlap population between the metal and O upon water adsorption is larger on Ru (0.71) than on Pt (0.56) in the alloy. This accounts for the stronger H₂O adsorption on the Ru site which is reflected by a larger binding energy (see Table 2). For the pure Pt, the DOS curves of these interactions (Figure 6a and b) take on the shape of Figure 7a and b. One observes by comparing Figures 6b and 7b that the stabilization interaction of d_{yz} Pt orbital with $1b_2$ is weaker in the Pt-Ru alloy than in pure Pt because the rise of the Fermi level leads to more occupied antibonding states and the less electron donation of $1b_2$ (0.14 vs. 0.22 e^- in Table 2) in the case of the alloy. This point is further illustrated by the COOP curves of

Figures 6c-8c. Note the antibonding peak that is close to the Fermi level besides the bonding peaks at low energy. The antibonding combination of p_y (O) with d_{yz} (Ru) is totally destabilized above the Fermi level but that of p_y (O) with d_{yz} (Pt) is not; the latter case is responsible for a closed-shell repulsive interaction accompanying small stabilization. If the d band of the metal atoms directly involved in the adsorption is farther from E_F , as is the case for Pt in the alloy, a larger part remains below it and a closed-shell repulsive interaction is stronger. In this case, less electronic charge will be dumped from the antibonding counterpart orbitals at the Fermi level, thereby weakening the effect of the donation stabilization.

For the systems studied, the decrease in the binding energy of the H₂O adsorption is essentially due to an increase of the closed-shell repulsive interactions between H₂O and the surface. The electron transfer between H₂O and the surface follows the same trend. The electron loss of the lone-pair orbitals results from the interaction destabilizing some of their electronic states above the Fermi level. Therefore the donations from H₂O to the surface decrease with increasing repulsive interactions between them. With this in mind, we can deduce from Table 2 that the increased H₂O adsorption energy correlates with an increased H₂O charge.

Discussion and Conclusions

We have shown that a substitutional Ru atom in a Pt(111) surface donates electron density to the surface Pt atoms and becomes a good acceptor of electron density from water molecules. Compared to the pure Pt, the surface Pt atoms in the Pt-Ru alloy are more negatively charged because of an electron transfer from Ru to Pt. Surprisingly, a better electron gain is induced for the Pt atoms that have no Ru as neighbor. The Fermi level of the alloy is higher than that of the pure Pt. The DOS peaks projected on d orbitals are somewhat narrower in the alloy: the d band well-localized on Ru being located at and near the Fermi level and that on Pt farther from this level. A substitutional Ru atom is calculated to bind H₂O preferentially. Lone-pair donation bonding is the dominant water-surface interaction. The strong donation interaction with Ru is due to the presence of the empty d orbitals well-localized on Ru near the Fermi level since all antibonding combinations are left vacant. The Pt site in the alloy binds H₂O less strongly than the Ru site. The weaker bonding to the Pt atom can be understood in terms of the larger repulsive interactions. Since the d bands of Pt atoms in the alloy are farther below the Fermi level, these d bands are less pushed above the Fermi level by their interactions with water lone-pair and more occupied states participate in the destabilizing component giving rise to repulsions.

The substitutional Ru atom was found to be more active toward H₂O decomposition to OH(ads) than the Pt atoms.¹³ The calculations showed that the strong activation for OH bond cleavage is linked to the strong donation bonding of water. This was proposed as the explanation for the well-known²² ability of Pt-Ru alloys to catalyze the oxidation of

the CO poison on fuel cell anodes; that is, OH(ads) was found to be a viable oxidant, yielding $\text{CO}_2 + \text{H}^+ + \text{e}^-$. Our calculations show in Table 2 that the O-H overlap population does not vary much from its value in free H_2O when the water adsorption takes place on Ru in the Pt alloy. Consequently, the electron donation from H_2O lone-pair orbitals does not contribute to weakening the O-H bonds, since they are of nonbonding character. So we suggest that the substitutional surface Ru atoms in the Pt electrode attract water molecules and activate OH(ads) formation at a higher anode potential. An increasingly anodic surface potential can be modeled by decreasing the metal s, p, and d diagonal Hamiltonian matrix elements (H_{ii}). When the potential of the electrode is increased by 1 V, the electrode surface valence band is stabilized by approximately 1 eV. As the metal valence band moves down by decreasing the metal H_{ii} values, its bottom becomes close to the low-lying H_2O $1b_1$ orbital in energy and hence its stabilization is expected to be larger due to stronger mixing with the metal d band orbitals. This stronger OH σ donation bonding to the surface seems to be responsible for the catalytic effect of Ru in the alloy on activating the formation of OH (ads) at higher potentials. We find that the O-H overlap population is reduced (0.64 to 0.59) for H_2O bound to Ru in the alloy when the surface potential is increased by 1 V relative to the 0 V parameters in Table 1. This means that the O-H bond becomes weaker and has a tendency to break as the potential increases. Whether or not Ru in the alloy would activate the water dissociation should be explored further because there is no correlation between the adsorption energy and the activation energy of H_2O .

Appendix

For the periodic calculations, the tight-binding EH method has been applied.²³ A mesh of 66 k points was chosen in the irreducible part of the Brillouin zone for the average property calculations. The EHMO cluster calculations were performed with the help of YAeHMOP program developed by G. Landrum.²⁴

References

1. Debauge, Y.; Abon, M.; Bertolini, J. C.; Massardier, J.; Rochefort, A. *Appl. Surf. Sci.* **1995**, *90*, 15.
2. Hamdaoui, A. El.; Bergeret, G.; Massardier, J.; Primet, M.; Renouprez, A. *J. Catal.* **1994**, *148*, 47.
3. (a) Xu, C.; Koel, B. E.; Paffett, M. T. *Langmuir* **1994**, *10*, 166. (b) Xu, C.; Tsai, Y.-L.; Koel, B. E. *J. Phys. Chem.* **1994**, *98*, 585.
4. Xu, C.; Koel, B. E. *Surf. Sci.* **1994**, *310*, 198.
5. Paffett, M. T.; Gebhard, S. C.; Windham, R. G.; Koel, B. E. *J. Phys. Chem.* **1990**, *94*, 6831.
6. Atli, A.; Abon, M.; Beccat, P.; Bertolini, J. C.; Tardy, B. *Surf. Sci.* **1994**, *302*, 121.
7. Rochefort, A.; Abon, M.; Delichere, P.; Bertolini, J. C. *Surf. Sci.* **1993**, *294*, 43.
8. Atli, A.; Abon, M.; Bertolini, J. C. *Surf. Sci.* **1993**, *287-288*, 110.
9. Marinelli, T. B. L. W.; Nabuurs, S.; Ponec, V. *J. Catal.* **1995**, *151*, 431.
10. Beccat, P.; Bertolini, J. C.; Gauthier, Y.; Massardier, J.; Ruiz, P. *J. Catal.* **1990**, *126*, 451.
11. Bertolini, J. C.; Massardier, J. *Catal. Lett.* **1991**, *9*, 183.
12. Borgna, A.; Moraweck, B.; Massardier, J.; Renouprez, A. *J. Catal.* **1991**, *128*, 99.
13. Anderson, A. B.; Grantscharova, E. *J. Phys. Chem.* **1995**, *99*, 9149.
14. *Tables of Parameters for Extended Hückel Calculations*; collected by Alvarez, S., Universitat de Barcelona, 1995.
15. An adjusted set of H_{ii} values is based on the valence state ionization potentials (VSIPs) determined by Lotz and Moore from spectroscopic data. See: Lotz, W. *J. Opt. Soc. Am.* **1970**, *60*, 206; Moore, C. E. *Atomic Energy Levels*; Natl. Bur. Std. (U.S.); U.S. Govt. Printing Office: Washington, DC, 1949; Vol. 1, 1952; Vol. 2, 1958; Vol. 3.
16. Wagner, F. T.; Moylan, T. E. *Proc. Electrochem. Soc.* **1992**, *92(11)*, 25.
17. Kizhakevariam, N.; Stuve, E. M. *Surf. Sci.* **1992**, *275*, 223.
18. Ogasawara, H.; Yoshinobu, J.; Kawai, M. *Chem. Phys. Lett.* **1994**, *231*, 188.
19. Lee, T. R.; Whiteside, G. M. *J. Am. Chem. Soc.* **1991**, *113*, 2568.
20. Thiel, P. A.; Madey, T. E. *Surf. Sci. Rep.* **1987**, *7*, 211.
21. Anderson, A. B. *Surf. Sci.* **1981**, *105*, 159.
22. Gasteiger, H. A.; Markovic, N.; Ross, P. N.; Cairns, E. J. *J. Phys. Chem.* **1994**, *98*, 617; **1993**, *97*, 12020 and references therein.
23. Ren, J.; Liang, W.; Whangbo, M.-H. *Crystal and Electronic Structure Analyzer*; 1998. For details, see: <http://www.PrimeC.com/>.
24. Landrum, G. A. *Yet Another extended Hückel Molecular Orbital Package*; <http://overlap.chem.cornell.edu:8080/yaehmop.html>, 1997.